CHAPTER 8

DIOSCOREA BULBIFERA EXTRACT: NATURAL CORROSION INHIBITOR FOR MILD STEEL IN ACID MEDIA

This chapter explores the potent corrosion inhibition property of green *Dioscorea bulbifera* leaf extract (DBE) on the mild steel in 1 M HCl and 0.5 M H_2SO_4 using physicochemical, electrochemical and surface morphological techniques. Even though DBE contains myriads of phytochemical constituents, three essential chemical components, bafoudiosbulbin A, diosgenin and kaempferol[196], have been subjected to quantum mechanical studies to supplement the corrosion inhibition mechanism of the leaf extract in more detail. Its structures are shown in Fig. 8.1.

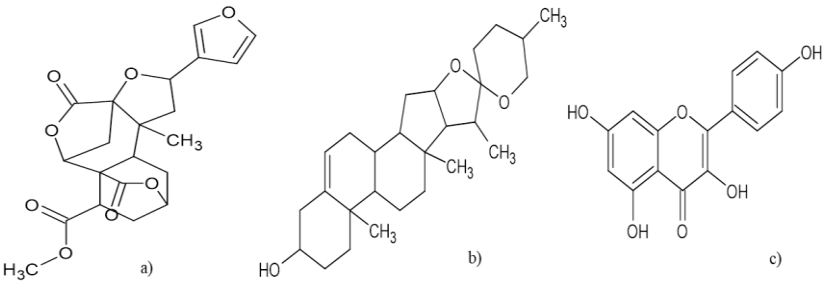

Fig. 8.1: Structures of a) bafoudiosbulbin A b) diosgenin c) kaempferol

Dioscorea bulbifera

Results and discussions

Phytochemical screening of DBE

Standard qualitative identification tests were performed to detect the phytochemicals present in DBE, and the observations are given in Table 8.1.

FTIR spectroscopy

Chemical structure and functional groups of DBE can be evaluated using FTIR spectroscopy (Fig. 8.2). An intensive and broad absorption peak at 3281 cm^{-1}, designating -OH functional groups in DBE molecules. The peak found at 2917 cm^{-1} is represented by alkyl C-H bond vibration. >C=O stretching vibration was observed at

1731 cm^{-1}. Aromatic C-C bond absorption peak was seen at 1610 cm^{-1}. Moreover, the weak peak seen at 1243 cm^{-1} corresponds to the absorption of C-O stretching vibration. In-plane bending of C-O-H was measured at 1403 cm^{-1} assigned to -COOH groups. The C-N stretching bond is seen at 1027 cm^{-1}. In short, the presence of an aromatic ring, -OH, >C=O and -COOH groups in the major chemical constituents of DBE was examined in the FTIR spectrum.

Table 8.1: Phytochemical screening of DBE

Sl. No.	Compounds	Tests	Results
1	Alkaloids	Mayer's reagent	−−
2	Steroids	Salkowaski's test	++
3	Phenolic compounds	Potassium ferrocyanide test	++
4	Flavanoids	Sodium hydroxide test	++
5	Saponins	Froth test	++
6	Tannins	Lead acetate test	−−
7	Cardiac glycosides	Conc. sulphuric acid test	++
8	Coumarin	Alcoholic NaOH test	++
9	Quinones	Conc. sulphuric acid test	++

++ (present), − − (Absent)

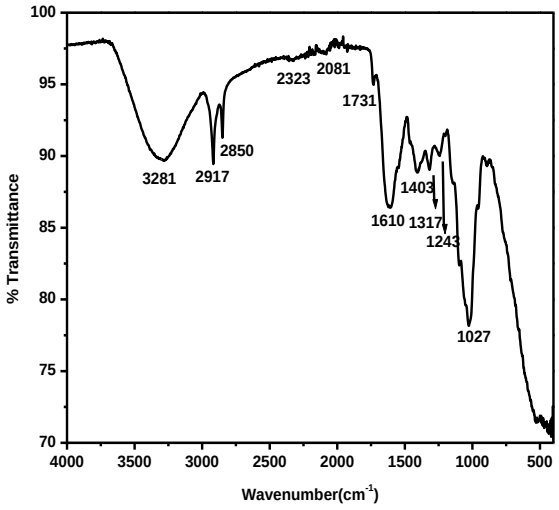

Fig. 8.2: FTIR spectrum of DBE

Weight loss measurements

Effect of concentration

According to Table 8.2, the corrosion rate (υ) of the metal treating without DBE as an inhibitor is much higher than the metals treating with DBE containing 1 M HCl and 0.5 M H_2SO_4 solutions. By increasing DBE concentration, the corrosion rate remarkably decreased. This diminution confirms the good inhibition effect of DBE. On close examination of Table 8.2, it was realized that after dissolving 5 v/v% DBE in 1 M HCl solution, the inhibition efficiency enhanced to 91.78%, whereas, in 0.5 M H_2SO_4 solution efficiency increased to 86.93%, clarifying the predominant protection power of DBE on mild steel exposed in HCl solution at room temperature[197].

Table 8.2: Weight loss measurements of mild steel with and without DBE in 1 M HCl and 0.5 M H_2SO_4 at room temperature for 24 hrs

Conc. (v/v%)	Corrosion rate (mm/yr)		Inhibition efficiency (η%)	
	1 M HCl	0.5 M H_2SO_4	1 M HCl	0.5 M H_2SO_4
Blank	3.95	35.57	-	-
1	1.16	17.69	70.52	50.26
2	0.93	16.02	76.34	54.94
3	0.72	14.03	81.53	60.55
4	0.65	12.31	83.48	65.38
5	0.32	4.648	91.78	86.93

❖ ***Effect of temperature***

Fig. 8.3 shows the comparison of inhibition efficiencies of mild steel in various concentrations of DBE in 1 M HCl and 0.5 M H_2SO_4 at different temperatures. From Fig. 8.3, it is noted that inhibition efficiency in HCl was higher than in H_2SO_4 at all temperatures under investigation. It claimed that the Cl^- ions tend to adsorb on the metal surface more quickly than SO_4^{2-} ions[64]. In HCl solution, inhibition efficiencies for all temperatures were in the range of 84-91%. The maximum inhibition efficiency was

found at 303 K for both acid media. The limited adsorbability of DBE molecules on the adsorbed SO_4^{2-} ions on the metal surface caused lower efficiency in the H_2SO_4 medium.

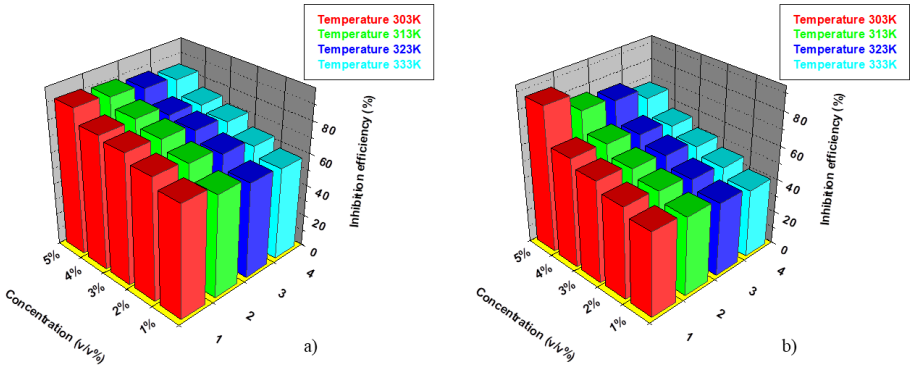

Fig. 8.3: Variation in inhibition efficiency of DBE in a) 1 M HCl b) 0.5 M H_2SO_4 at elevated temperatures

Table 8.3: Corrosion rate (υ) and inhibition efficiency (η%) of DBE in 1 M HCl and 0.5 M H_2SO_4 at different temperatures for 24 hrs

Medium	Conc. (v/v%)	υ (303 K)	η% (303 K)	υ (313 K)	η% (313 K)	υ (323 K)	η% (323 K)	υ (333 K)	η% (333 K)
1 M HCl	Blank	3.95	-	13.1	-	22.0	-	31.7	-
	1	1.16	70.5	4.66	64.3	8.79	60.1	13.2	58.3
	2	0.93	76.3	3.46	73.5	6.78	69.2	11.4	64.0
	3	0.72	81.5	2.66	79.6	5.40	75.5	8.99	71.6
	4	0.65	83.4	2.09	84.0	4.95	77.5	7.86	75.2
	5	0.32	91.7	1.32	89.8	2.90	86.8	4.99	84.2
0.5 M H_2SO_4	Blank	35.57	-	58.27	-	86.25	-	106.2	-
	1	17.69	50.26	30.73	47.25	48.15	44.17	62.65	41.04
	2	16.02	54.94	27.39	52.98	43.48	49.58	56.50	46.82
	3	14.03	60.55	24.69	57.62	38.04	55.89	51.06	51.94
	4	12.31	65.38	20.90	64.12	33.82	60.78	45.43	57.24
	5	4.648	86.93	13.86	76.21	22.56	73.84	34.60	67.43

Table 8.3 reveals that the corrosion rate significantly raised with increasing the operating temperature. This increase indicates that the mild steel dissolution rate can be signified at elevated temperatures[198]. For metals exposed to DBE containing HCl solutions, the corrosion rate lowered notably, elucidating that the DBE molecules could impressively retard the metal corrosion process.

The activation parameters can be reckoned by performing the weight loss measurements between 303 K and 333 K. The impact of temperature on mild steel corrosion in acid media with and without DBE was analyzed using Arrhenius and transition state equations (Eqs. (41) and (43)). Arrhenius and transition state plots are pictorially represented in Fig. 8.4 and Fig. 8.5 in 1 M HCl and 0.5 M H_2SO_4, respectively, and the obtained parameters are summarized in Table 8.4.

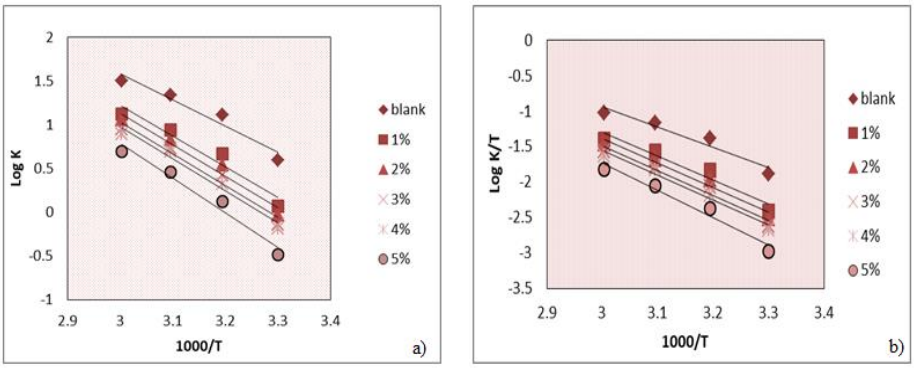

Fig. 8.4: Arrhenius plots of a) log K vs 1000/T b) log K/T vs 1000/T with and without DBE in 1 M HCl

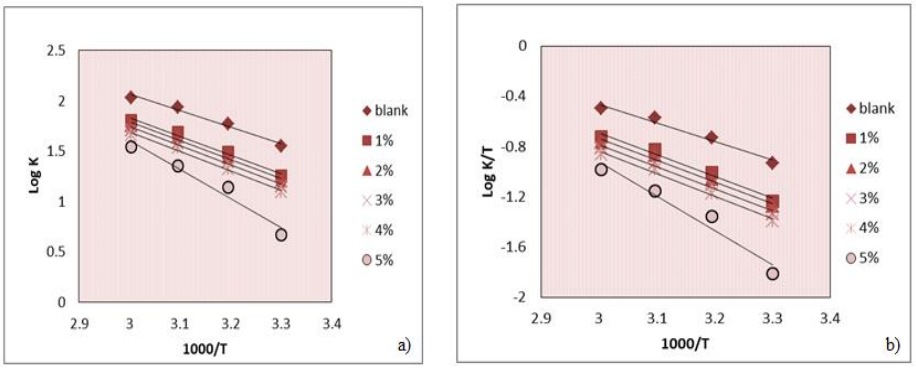

Fig. 8.5: Arrhenius plots of a) log K vs 1000/T b) log K/T vs 1000/T with and without DBE in 0.5 M H_2SO_4

On inspection of Table 8.4, it was clear that in the presence of DBE, the activation energy values shifted to higher values compared with uninhibited metal. It can be ascribed to the adsorption of DBE molecules on the mild steel surface through the physisorption mechanism. Activation parameters illustrated that the activation enthalpy (ΔH^*) and entropy (ΔS^*) values became more positive by enhancing the DBE

concentration. The positive values of ΔH* mention the endothermic process of mild steel corrosion. At the same time, ΔS* values progressed to be less negative, implies the disorderliness of DBE molecules enhancement.

Table 8.4: Thermodynamic parameters of mild steel corrosion with and without DBE in 1 M HCl and 0.5 M H_2SO_4

Medium	Conc. (v/v %)	E_a (kJ mol^{-1})	A	ΔH^* (kJ mol^{-1})	ΔS^* (J $mol^{-1}K^{-1}$)
1 M HCl	Blank	57.24	3.58×10^{10}	54.61	-44.7842
	1	66.98	5.18×10^{11}	64.34	-22.5410
	2	69.03	8.41×10^{11}	66.39	-18.5315
	3	69.51	8.95×10^{11}	66.87	-18.0203
	4	70.19	9.44×10^{11}	67.56	-17.5684
	5	75.76	4.54×10^{12}	73.12	-4.4890
0.5 M H_2SO_4	Blank	30.96	8.16×10^{6}	28.32	-114.510
	1	35.71	2.68×10^{7}	33.08	-105.524
	2	35.72	2.40×10^{7}	33.62	-104.783
	3	36.26	2.63×10^{7}	33.81	-104.628
	4	36.99	3.04×10^{7}	34.35	-103.567
	5	54.93	1.61×10^{10}	52.29	-51.378

Adsorption isotherms

Effectiveness of the adsorption of inhibitor molecules on the mild steel surface was explained by adsorption isotherm. The mechanism of inhibition by adsorption was investigated by considering various adsorption isotherms such as Langmuir, El-Awady, Frumkin, Temkin, Freundlich and Flory-Huggins isotherms. Eqs. (34)–(40) were applied for a suitable fitting. Among the isotherms, the best adsorption isotherm was Langmuir isotherm for 1 M HCl whereas, it was Frumkin isotherm for 0.5 M H_2SO_4 based on the closeness of linearity index to unity. It can be found from Fig. 8.6 a) and Fig. 8.6 b) straight line with R^2=0.9911 and R^2=0.9267 for HCl and H_2SO_4 media, respectively. Furthermore, the adsorption constant (K_{ads}) was computed. Greater the values of K_{ads} declare that the DBE molecules adsorption on the mild steel happens instinctively[82].

The observed values of ΔG_{ads}° and K_{ads} are shown in Table 8.5. The examined negative values of ΔG_{ads}° evidence that the DBE molecules effectively adsorbed on the mild steel surface. Results obtained in Table 8.5 reveals that ΔG_{ads}° value was more negative for HCl medium than H_2SO_4 medium. Current works reported that the ΔG_{ads}° values between −28 to −38 $kJ \cdot mol^{-1}$ represent the mixed type of adsorption mode by inhibitor molecules, i.e., physical and chemical adsorption. So, here DBE molecules adsorbed on the mild steel surface via physical and chemical adsorption mechanisms.

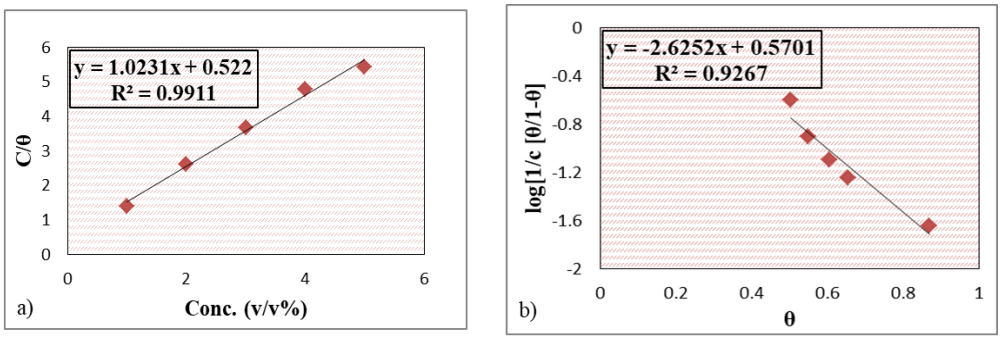

Fig. 8.6: a) Langmuir adsorption isotherm of DBE on mild steel in 1 M HCl and b) Frumkin adsorption isotherm of DBE on mild steel in 0.5 M H_2SO_4

Table 8.5: Adsorption parameters of mild steel in 1 M HCl and 0.5 M H_2SO_4 with DBE from weight loss measurements at room temperature

Medium	ΔG_{ads}^{0} ($kJmol^{-1}$)	K_{ads}	R^2
1 M HCl	28.96	1915.70	0.9911
0.5 M H_2SO_4	28.74	1754.07	0.9267

Electrochemical impedance spectroscopy

EIS illustrated the electrochemical characteristics of the mild steel exposed to 1 M HCl and 0.5 M H_2SO_4 solutions containing DBE. Fig. 8.7 and Fig. 8.8 represent Nyquist and Bode plots of metals exposed to acid solutions with and without DBE after 30 seconds of immersion. Nyquist plots displayed one capacitive semicircle, defining that the charge transfer process chiefly controls mild steel corrosion. Observing Fig. 8.7, Nyquist plots of metals dipped in acid solutions without DBE exhibited semicircles with much smaller diameters than metals subjected to acid solutions containing DBE. It has

been noticed that by enhancing the concentration of DBE, the Nyquist plot diameter becomes more extensive.

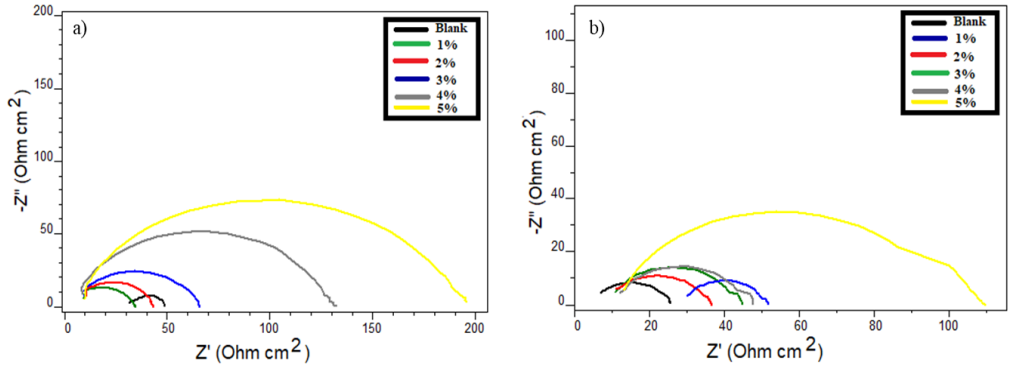

Fig. 8.7: Nyquist plots of mild steel with and without DBE in a) 1 M HCl and b) 0.5 M H_2SO_4

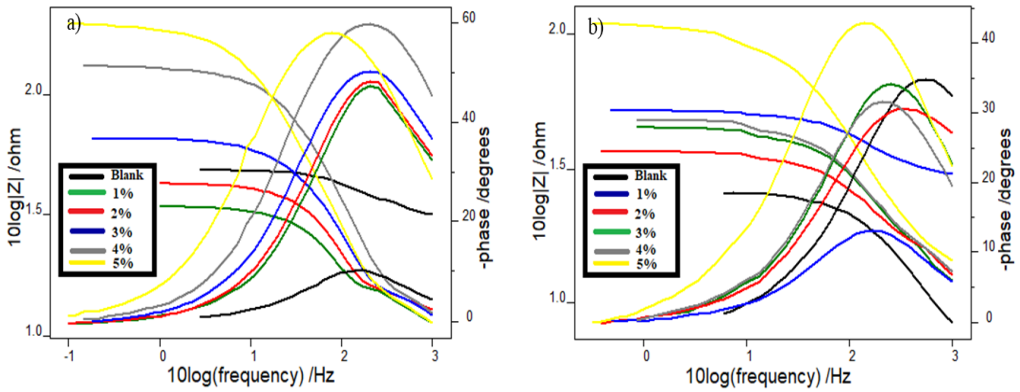

Fig. 8.8: Bode plots of mild steel with and without DBE in a) 1 M HCl and b) 0.5 M H_2SO_4

Table 8.6: Impedance parameters of mild steel in 1 M HCl and 0.5 M H_2SO_4 with and without DBE

Conc. (v/v %)	1 M HCl			0.5 M H_2SO_4		
	R_{ct} (Ωcm^2)	C_{dl} (μFcm^{-2})	η_{EIS}%	R_{ct} (Ωcm^2)	C_{dl} (μFcm^{-2})	η_{EIS}%
Blank	15.7	78.8	-	18.1	47.4	-
1	42.0	74.2	62.61	33.6	46.8	46.13
2	54.1	69.3	70.97	36.4	44.1	50.27
3	63.4	62.4	75.23	39.1	43.9	53.70
4	115	53.7	86.34	42.5	43.3	57.41
5	170	40.1	90.76	85.1	39.2	78.73

The electrochemical parameters derived from Nyquist and Bode plots fitted by suitable equivalent circuits (Randle's equivalent circuit) are tabulated in Table 8.6. On close examination of Table 8.6 revealed that by increasing DBE concentration, R_{ct} values

prominently increased, demonstrating DBE molecules adsorption on the mild steel surface. Moreover, double-layer capacitance (C_{dl}) values were estimated by maintaining a constant phase element. Table 8.6 reveals that with raising DBE concentration, C_{dl} values diminished, clarifying the local dielectric thickness depletion and the water molecules substitution with DBE molecules[199]. These observations made that DBE molecules can strongly retard the mild steel corrosion rate in 1 M HCl and 0.5 M H_2SO_4. Inhibition efficiency of DBE reached 90.76% in 1 M HCl and 78.73% in 0.5 M H_2SO_4 for the maximum DBE concentration employed in this work.

Potentiodynamic polarization studies

Fig. 8.9 and Fig. 8.10 explains Tafel and linear polarization plots of mild steel, respectively, immersed in 1 M HCl and 0.5 M H_2SO_4 solutions containing various concentrations of DBE. Electrochemical parameters obtained from Tafel plots such as corrosion current density (i_{corr}), corrosion potential (E_{corr}), Tafel slopes (b_a and b_c) and that derived from linear polarization plots such as polarization resistance (R_p) and corresponding inhibition efficiencies calculated are given in Table 8.7. Tafel plots interpret that in the presence of DBE, both the anodic and cathodic curves were repositioned in the direction of lower current densities. It caused the blocking of active sites of the mild steel surface due to the adsorption of DBE molecules.

Changes in cathodic and anodic Tafel slopes are nearly comparable when the DBE molecules added to the acid media. Values of b_c and b_a indicated that the DBE adsorption on the mild steel surface changes both the cathodic and anodic branch shapes and slopes, suggesting that the hydrogen evolution and anodic dissolution mechanism controlled by DBE adsorption[168]. In addition, the shift in E_{corr} values concerning the blank metal is less than 85 mV declares the mixed inhibition effect of DBE.

The extreme inhibition capacity on mild steel surface was found by 5% DBE concentration in HCl and H_2SO_4 media as 91.69% and 87.31%. A similar trend was observed in weight loss and EIS studies that inhibition efficiency was minor in H_2SO_4 compared to HCl medium. Linear polarization studies also have maintained this observation.

The corrosion inhibition mechanism can be explained based on the role of DBE adsorption on the mild steel surface. The chemical interaction between organic molecules of DBE and the vacant 3d orbitals of the iron surface can change the iron dissolution mechanism and inhibit mild steel corrosion. Since the DBE molecules contain various functional groups with lone pair of electrons, they can interact with the anodic sites of the metal. As discussed earlier, i_{corr} values decreased with increasing DBE concentration, associated with cathodic reaction in the solution.

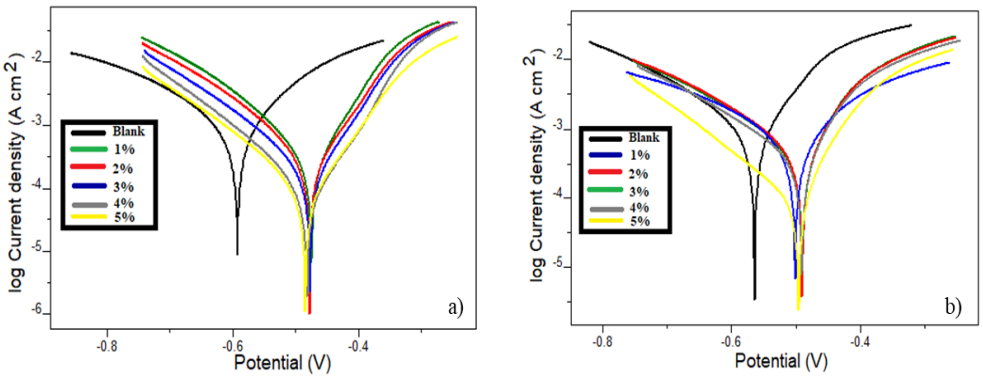

Fig. 8.9: Tafel plots of mild steel with and without DBE in a) 1 M HCl and b) 0.5 M H_2SO_4

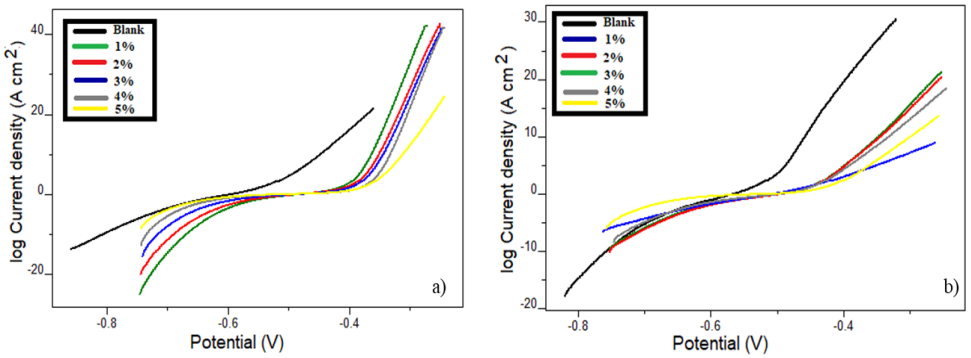

Fig. 8.10: Linear polarization plots of mild steel with and without DBE in a) 1 M HCl and b) 0.5 M H_2SO_4

Table 8.7: Potentiodynamic polarization parameters of mild steel in 1 M HCl and 0.5 M H_2SO_4 with and without DBE

Medium	Conc. (v/v %)	Tafel data				Polarization data		
		$-E_{corr}$ (mV)	i_{corr} (μAcm^2)	b_a (mV/dec)	$-b_c$ (mV/dec)	η_{pol}%	R_p (Ω)	η_{Rp}%
1 M HCl	Blank	597.9	1240	166	221	-	33.14	-
	1	529.0	430	110	146	65.32	91.15	63.64
	2	539.1	357	114	149	71.20	118.3	71.98
	3	553.6	231	98	147	81.37	129.25	74.35
	4	543.2	213	95	152	82.82	195.8	83.07
	5	546.5	103	111	159	91.69	274.0	87.90
0.5 M H_2SO_4	Blank	602.2	1616	184	193	-	25.30	-
	1	538.8	815	191	192	49.56	48.64	47.98
	2	519.5	762	227	258	52.84	51.36	50.73
	3	540.6	741	186	189	54.14	54.29	53.39
	4	551.2	685	200	184	57.61	58.51	56.75
	5	547.5	205	136	141	87.31	174.3	85.40

Electrochemical noise measurements

Shift in electrode potential is mainly used as a factor for determining pitting corrosion on mild steel. Fig. 8.11 exhibits the current noise spectra for mild steel treated with different DBE concentrations in 1 M HCl and 0.5 M H_2SO_4 solutions. It demonstrates that the current noise spectrum for metal treated without DBE was at higher amplitudes than metal dipped in DBE containing acid media reflecting adequate metal protection in the presence of DBE. PSD plots for metal fell in acid media with various DBE concentrations are portraited in Fig. 8.12. In PSD plots, when the frequency goes up, magnitudes of current noise get down. A similar observation can be seen in PSD plots as the current noise plots that the amplitudes of current for blank metal were higher than metal exposed in acid solutions with DBE. It declared metal dissolution prevention of DBE in acid media.

Pitting resistance equivalent number (PREN) is another term for the pitting index. Pitting index determines the capacity of an inhibitor to resist metal corrosion. Fig. 8.13 reveals pitting index curves for mild steel treated in acid solutions with and without DBE. Pitting index plots points out that in the presence of DBE, the pitting index value

was higher than that in the absence of DBE. Pitting index value was nobler for 5 v/v% DBE concentration in HCl medium, whereas it was lower in H_2SO_4 medium for a similar DBE concentration. Results showed that metal treated with DBE has good corrosion inhibition power in 1 M HCl and 0.5 M H_2SO_4. It also confirmed the better anti-corrosion property of DBE in 1 M HCl compared to 0.5 M H_2SO_4.

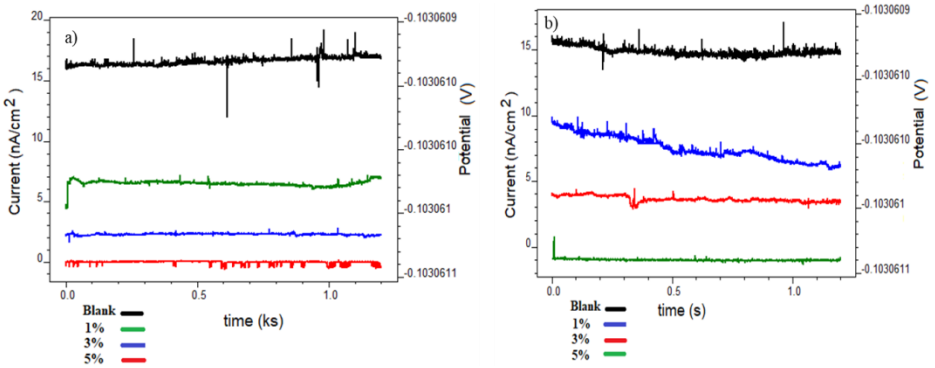

Fig. 8.11: Current noise plots of mild steel with and without DBE in a) 1 M HCl b) 0.5 M H_2SO_4

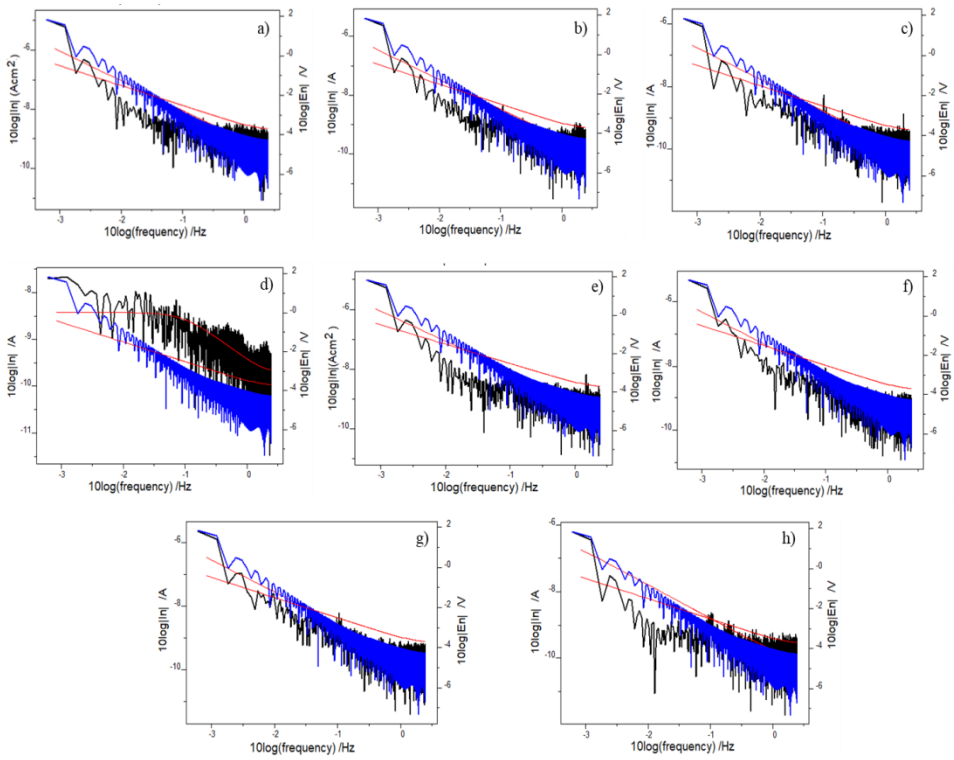

Fig. 8.12: Power spectral density plots of mild steel in 1 M HCl a) without DBE b) 1% DBE c) 3% DBE d) 5% DBE; Power spectral density plots of mild steel in 0.5 M H_2SO_4 e) without DBE f) 1% DBE g) 3% DBE h) 5% DBE

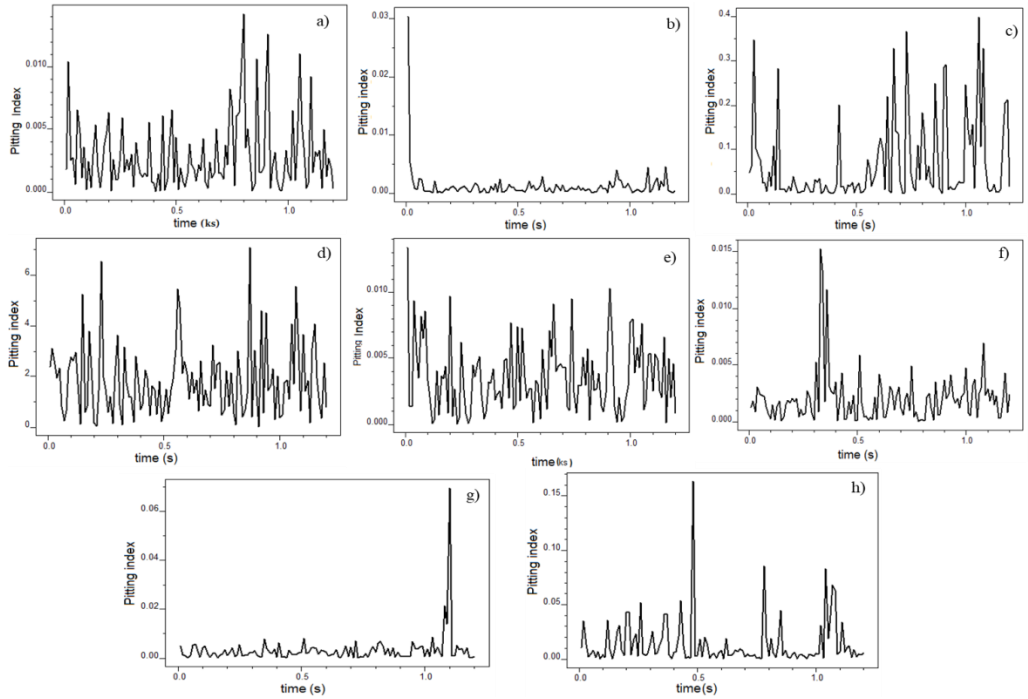

Fig. 8.13: Pitting index curves of mild steel in 1 M HCl a) without DBE b) 1% DBE c) 3% DBE d) 5% DBE; Pitting index curves of mild steel in 0.5 M H_2SO_4 e) without DBE f) 1% DBE g) 3% DBE h) 5% DBE

Scanning electron microscopy

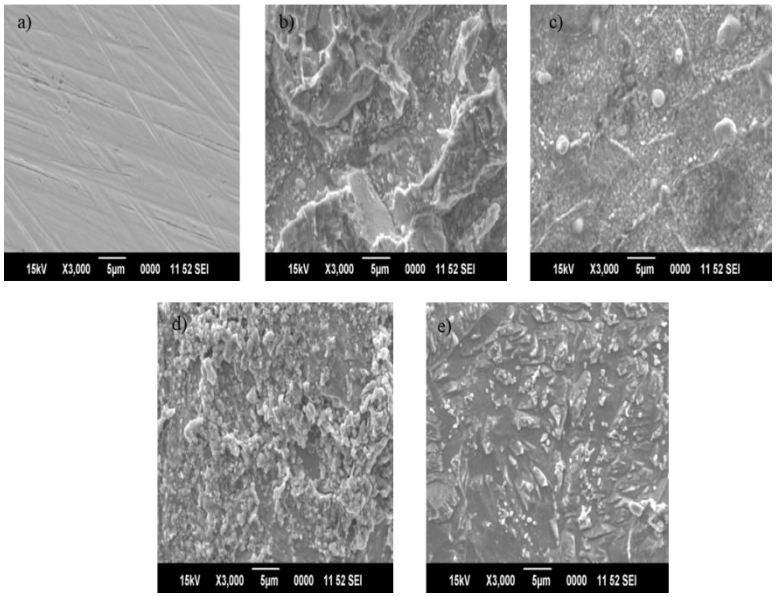

Fig. 8.14: SEM images of the surface of mild steel a) bare b) in 1 M HCl c) in 1 M HCl with DBE d) in 0.5 M H_2SO_4 e) in 0.5 M H_2SO_4 with DBE

Interaction mechanism between DBE molecules and mild steel can substantiate using SEM studies of metal coupons. Fig. 8.14 a) reveals the SEM image of the

smoothened surface of mild steel. SEM images of the surface of mild steel in 1 M HCl (Fig. 8.14 b & c) and 0.5 M H_2SO_4 (Fig. 8.14 d & e) were presented in the absence and presence of DBE, respectively. It showed that the lack of DBE severely damaged the surface of the mild steel. Also noticed that the metal destruction is predominant in the 0.5 M H_2SO_4 solution than in 1 M HCl solution. The metal surface became more refined and smooth in the presence of DBE molecules[188]. Therefore, it can be established that DBE behaves as an efficient corrosion inhibitor in acidic media.

Quantum mechanical calculations

According to the electronic perspective, donor-acceptor interactions cause the adsorption of inhibitors on the metal. Three important chemical constituents in the leaves of *Dioscorea bulbifera* are Bafoudiosbulbin A, Diosgenin and Kaempferol, which were subjected to quantum mechanical studies. From HOMO/LUMO plots and quantum mechanical parameters (Fig. 8.15 & Table 8.8), it is noted that the electron-rich centres of DBE molecules such as aromatic rings, double bonds and O heteroatoms could donate their electrons to proper nucleophiles or vacant orbitals of Fe atoms on mild steel. This electron donation of DBE molecules ensures their chemisorption.

Results showed that the ΔE value of the kaempferol was relatively lower than bafoudiosbulbin A and diosgenin, indicating a significant interaction of kaempferol molecules with the mild steel surface. Thus better electron donation of kaempferol results in improved inhibition capacity of DBE molecules. The presence of hydroxyl groups in aromatic rings enhances the electron-donating ability of kaempferol. The order of ΔE values of the components was kaempferol (4.155 eV) < bafoudiosbulbin A (5.171 eV) < diosgenin (5.249 eV).

Lower electronegativity (χ) of kaempferol (1.0245) supports the transfer of electrons to metals which having higher electronegativity. The number of electrons

transferred (ΔN) also determine the electron donation power of inhibitor molecules[53]. ΔN values of molecules in the order of kaempferol (1.43) > bafoudiosbulbin A (1.057) >diosgenin (1.05). All the values are less than 3.6, which leads to efficient metal corrosion inhibition.

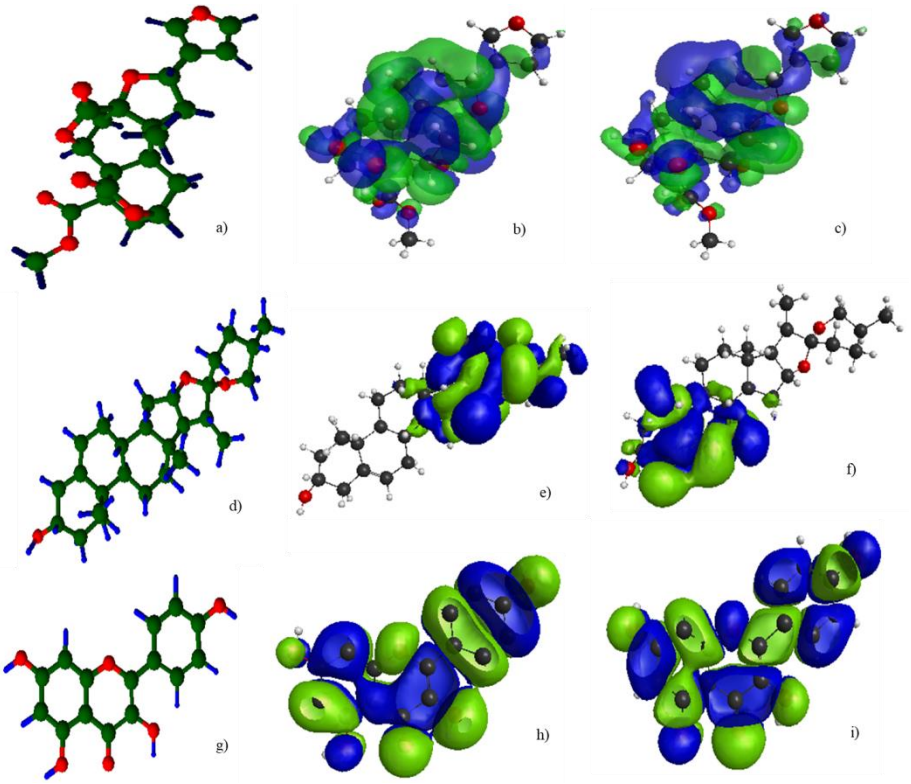

Fig. 8.15: a) Optimized geometry, b) HOMO and c) LUMO of bafoudiosbulbin A; d) Optimized geometry, e) HOMO and f) LUMO of diosgenin; g) Optimized geometry, h) HOMO and i) LUMO of kaempferol

Table 8.8: Quantum mechanical parameters (in eV) of bafoudiosbulbin A (I), diosgenin (II) and kaempferol (III)

Molecule	E_{HOMO}	E_{LUMO}	ΔE	I	A	μ	χ	η	ΔN
I	-4.118	1.053	5.171	4.118	-1.053	-1.53	1.53	2.58	1.057
II	-4.112	1.137	5.249	4.112	-1.137	-1.48	1.48	2.62	1.050
III	-3.102	1.053	4.155	3.102	-1.053	-1.02	1.02	2.07	1.438

Statistical analysis

❖ ***Optimization of factors for inhibition efficiency (IE%)***

Experimental results disclosed three predominant factors, i.e., temperature, DBE concentration, and acid concentration which affected the corrosion inhibition efficiency.

So they opted as independent factors for statistical analysis. Weight loss studies revealed that the corrosion rate was improved in H_2SO_4 than in HCl medium. So, HCl concentration was selected as an acid concentration. The structure of the design and the three levels of BBD are shown in Table 8.9, including experimental results and predicted response. A total of 15 experimental runs were performed in it. To identify the proper combination of the three factors used in this analysis for obtaining the highest efficiency, RSM was employed as an optimization technique. The regression model satisfying the test factors and the inhibition efficiency is given in equation (58).

$$IE = 379 - 1.36\ X_1 + 7.3\ X_2 - 52.0\ X_3 + 0.0011\ X_1^2 - 0.350\ X_2^2 - 14.35\ X_3^2 + 0.0060\ X_1X_2 + 0.217\ X_1X_3 - 0.83\ X_2X_3 \quad (58)$$

This full quadratic model was used to perform analysis of variance (ANOVA)[200]. ANOVA results with a significance level of 95% are demonstrated in Table 8.10. P-value is the most remarkable parameter in this Table. P-value predicts whether the impact of a factor on response significant or not. The degree of essentialness (α) was chosen to be 0.05. Results showed that P-value was lower than 0.05 for all the linear and one of the square terms. It explained that temperature, DBE concentration, HCl concentration and square term of HCl concentration were significant factors. The same results were obtained in Pareto chart (Fig. 8.16). It illustrates that DBE concentration has the most appreciable impact on the inhibition efficiency. Squared terms of temperature and DBE concentration were observed to influence the inhibition efficiency (IE%) negatively. Similarly, the interaction terms X_1X_3, X_1X_2 and X_2X_3 did not impact inhibition efficiency.

The suitable fit model for experimental results verified by the closeness of R^2 and R^2(adj) value to unity. Here, the R^2 and R^2(adj) values were 0.9888 and 0.9686,

respectively, suggesting the best-fit regression model for experimental values. Therefore, the results can be evaluated by this full quadratic model.

Table 8.9: Experimental and predicted IE% from weight loss measurements and BBD

Run order	Actual level of factors			IE%		Residual
	X_1	X_2	X_3	Experimental	Predicted	
1	323	3	1	75.51	80.29	4.7869
2	323	1	1.5	53.06	56.97	3.9139
3	313	5	1	89.87	95.64	5.7769
4	333	3	1.5	60.17	67.21	7.0409
5	323	1	0.5	63.48	68.41	4.9329
6	323	3	1	75.51	80.29	4.7869
7	333	5	1	84.28	87.59	3.3189
8	333	3	0.5	72.08	78.13	6.0599
9	323	3	1	75.51	80.29	4.7869
10	313	3	0.5	86.06	88.59	2.5379
11	323	5	0.5	89.65	95.30	5.6549
12	313	1	1	64.39	70.65	6.2649
13	313	3	1.5	69.81	73.32	3.5189
14	333	1	1	58.32	62.12	3.8069
15	323	5	1.5	75.9	80.54	4.6459

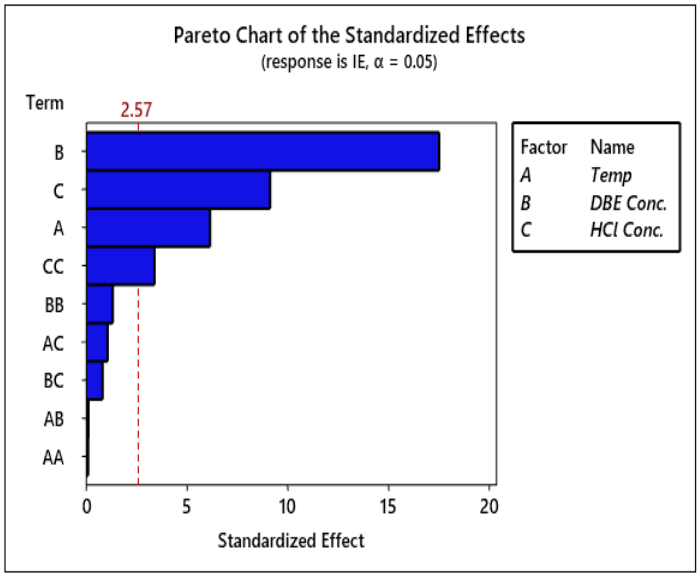

Fig. 8.16: Pareto chart of the standardized effects of mild steel

Main effects plots indicate the influence of tested factors on the response. Fig. 8.17 elucidates the main effects plots for the fitted means of inhibition efficiency. It revealed that the highest inhibition efficiency was found for 5 v/v% concentration of

DBE at a working temperature of 313 K at 0.5 M concentration of HCl. Kinetic energy of DBE molecules and the speed of bombardment between the molecules increases at higher temperatures. This trend prevents and destroys the formation of adsorbed film by inhibitors on the metal surface. So, at elevated temperatures, inhibition efficiency decreases.

Table 8.10: Analysis of variance for corrosion inhibition efficiency

Source	DF	Adj SS	Adj MS	F-Value	P-Value
Model	9	1819.69	202.19	49.05	0.000
Linear	3	1759.16	586.39	142.27	0.000
Temp	1	155.58	155.58	37.75	0.002
DBE Conc.	1	1261.28	1261.28	306.01	0.000
HCl Conc.	1	342.30	342.30	83.05	0.000
Square	3	52.99	17.66	4.29	0.076
Temp*Temp	1	0.04	0.04	0.01	0.924
DBE Conc.*DBE Conc.	1	7.25	7.25	1.76	0.242
HCl Conc.*HCl Conc.	1	47.49	47.49	11.52	0.019
2-Way Interaction	3	7.54	2.51	0.61	0.637
Temp*DBE Conc.	1	0.06	0.06	0.01	0.910
Temp*HCl Conc.	1	4.71	4.71	1.14	0.334
DBE Conc.*HCl Conc.	1	2.77	2.77	0.67	0.449
Error	5	20.61	4.12		
Lack-of-Fit	3	20.61	6.87	*	*
Pure Error	2	0.00	0.00		
Total	14	1840.30			

DF: degrees of freedom, Adj SS: adjusted sum of squares, Adj MS: adjusted mean of squares, F: Fischer's F-test value, P: probability

Similarly, when HCl concentration raised from 0.5 M to 1.5 M, inhibition efficiency decreased. In contrast, inhibition power was directly proportional to DBE concentration. The corrosion rate was tremendously boosted in the absence of an inhibitor and dropped when the inhibitor was present. Thus, the adsorption of inhibitor molecules enhances, and efficiency also increases.

Accuracy of this full quadratic equation (58) can be interpreted from residual plots given in Fig. 8.18. It consists of four different plots. Normal probability plot observed that this full quadratic equation for inhibition efficiency was fixed to the normal distribution. It indicated that the obtained model required no response transformation.

Versus fits plot revealed that the range of variance of observations was constant for all responses. Histogram of residuals pointed out that the residuals were allocated symmetrically for all frequencies. The fine uniform shape of this histogram validates the accuracy of the regression model. Versus order plot exhibited that points of observed runs were scattered randomly, keeping the fixed area of residuals which substantiated the model's precision. In conclusion, all four plots confirmed the accuracy of the model to demonstrate the influence of factors on the inhibition efficiency.

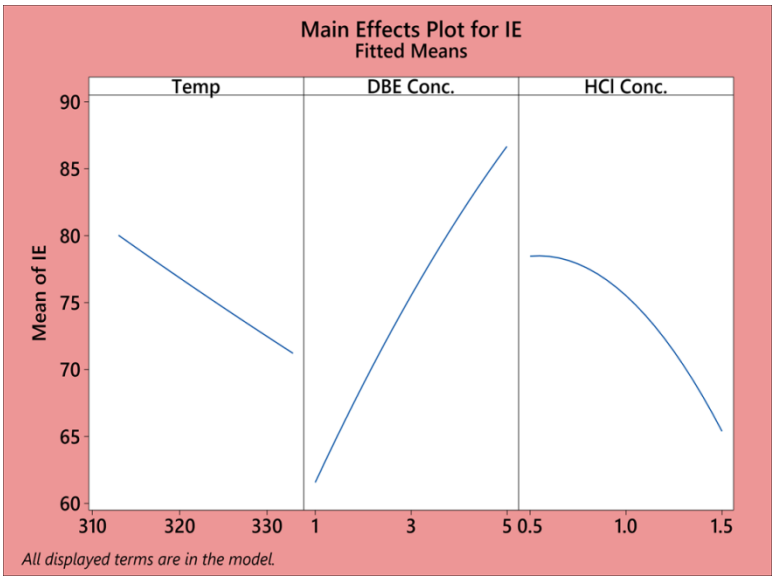

Fig. 8.17: Main effects plots for inhibition efficiency of mild steel in HCl medium

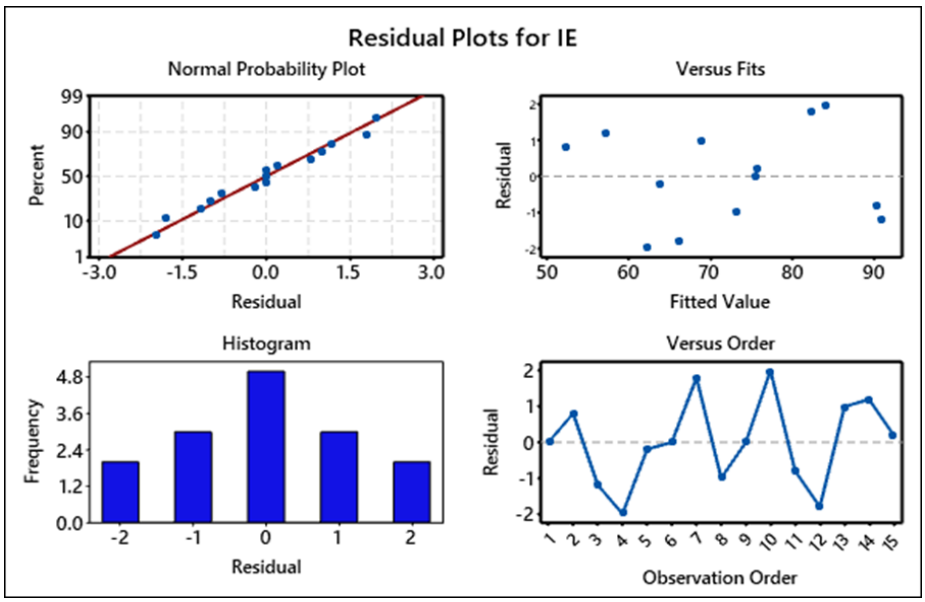

Fig. 8.18: Residual plots for inhibition efficiency

Contours and 3-D surface plots describe the inter-dependence of the tested factors on IE% and are shown in Fig. 8.19. It was realized that IE% goes up when DBE concentration rises for a given temperature. But, inhibition efficiency and temperature have an inverse relationship. This inclination can be attributed to the physical adsorption of DBE molecules on the mild steel surface. Because, as temperature rises, the rate of desorption increases. Similarly, inhibition efficiency and HCl concentration are inversely proportional.

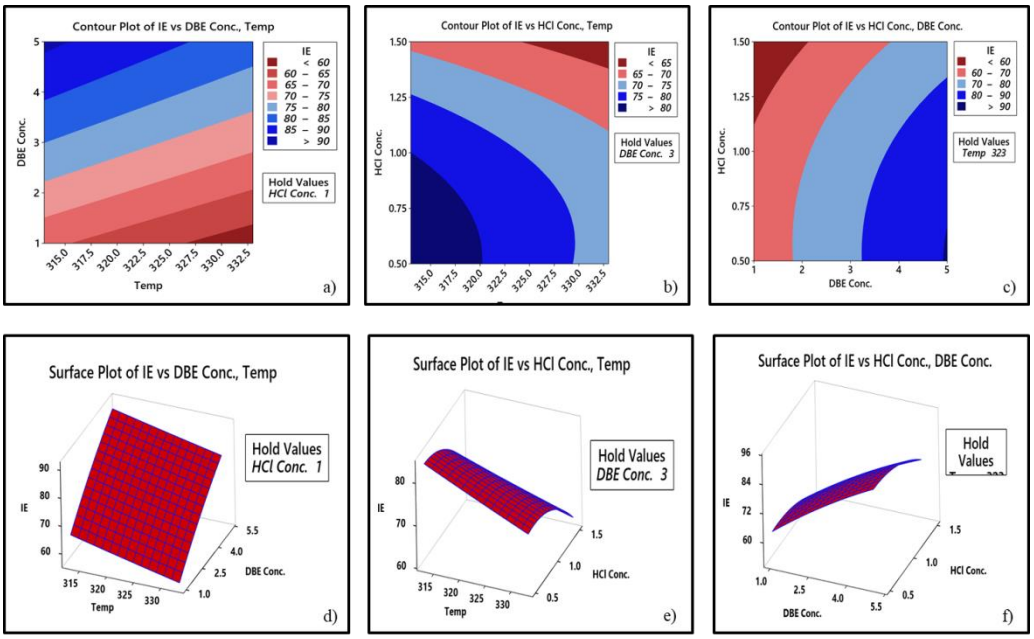

Fig. 8.19: a, b & c) Contours and d, e & f) 3-D surface plots for inhibition efficiency

❖ ***Response optimization***

A well-organized numerical model in quadratic equation (58) was applied to optimize the independent factors such as temperature, DBE concentration, and HCl concentration to achieve the maximum IE%. Desirability function method was employed for optimization. Response optimization plot for IE% is exhibited in Fig. 8.20. The optimum conditions for best IE% were temperature (313 K), DBE concentration (5 v/v %), and HCl concentration (0.5 M) and the corresponding predicted IE% was

95.9337%, as shown in Fig. 8.20. This optimization technique helped to verify the recurrence of the experimental outcomes and approve the validity of the model.

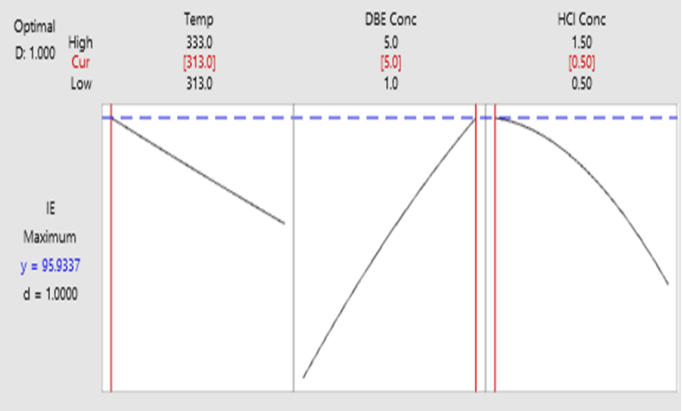

Fig. 8.20: Response optimization plot for inhibition efficiency

Conclusions

- DBE was found to be an efficient corrosion inhibitor for mild steel corrosion exposed in 1 M HCl and 0.5 M H_2SO_4.
- Weight loss studies exhibited that increasing the DBE concentration leads to an increase in inhibition efficiency. It is due to the adsorption of DBE molecules on the metal surface. In comparison, at higher temperatures, inhibition potential reduces due to the desorption of the adsorbed layer.
- Maximum inhibition capacity of DBE in 1 M HCl and 0.5 M H_2SO_4 was estimated as 91.78% and 86.93%, respectively.
- Langmuir adsorption isotherm was identified as good adsorption of DBE molecules on mild steel surface in HCl medium, while Frumkin was the best isotherm in the H_2SO_4 medium.
- Surface morphology of mild steel was studied by SEM, which supplemented strong evidence for forming a protective film on mild steel with DBE in acidic environments.

- Quantum mechanical calculations of three important phytochemicals were also supported the good inhibition efficiency of DBE.
- Response surface methodology was applied to validate the interdependence between DBE concentration, HCl concentration, and temperature on the inhibition efficiency by designing BBD. Regression equation could describe the results obtained from experiments in good agreement.